Cerebral Cortex, November 2016;26: 3705–3718

doi:10.1093/cercor/bhv168
Advance Access Publication Date: 6 August 2015
Original Article

ORIGINAL ARTICLE

Mutation of the Dyslexia-Associated Gene *Dcdc2* Enhances Glutamatergic Synaptic Transmission Between Layer 4 Neurons in Mouse Neocortex

Alicia Che[1,3], Dongnhu T. Truong[2,4], R. Holly Fitch[2] and Joseph J. LoTurco[1]

[1]Department of Physiology and Neurobiology, [2]Department of Psychology, University of Connecticut, Storrs, CT 06269, USA, [3]Current address: Weill Cornell Medical College, Brain & Mind Research Institute, New York, NY 10021, USA and [4]Current address: Department of Pediatrics, Yale University, New Haven, CT 06520, USA

Address correspondence to Dr Joe LoTurco, Department of Physiology and Neurobiology, University of Connecticut, Storrs, CT 06269-3156, USA.
Email: joseph.loturco@uconn.edu

Abstract

Variants in *DCDC2* have been associated with reading disability in humans, and targeted mutation of *Dcdc2* in mice causes impairments in both learning and sensory processing. In this study, we sought to determine whether *Dcdc2* mutation affects functional synaptic circuitry in neocortex. We found mutation in *Dcdc2* resulted in elevated spontaneous and evoked glutamate release from neurons in somatosensory cortex. The probability of release was decreased to wild-type level by acute application of *N*-methyl-D-aspartate receptor (NMDAR) antagonists when postsynaptic NMDARs were blocked by intracellular MK-801, and could not be explained by elevated ambient glutamate, suggesting altered, nonpostsynaptic NMDAR activation in the mutants. In addition, we determined that the increased excitatory transmission was present at layer 4–layer 4 but not thalamocortical connections in *Dcdc2* mutants, and larger evoked synaptic release appeared to enhance the NMDAR-mediated effect. These results demonstrate an NMDAR activation-gated, increased functional excitatory connectivity between layer 4 lateral connections in somatosensory neocortex of the mutants, providing support for potential changes in cortical connectivity and activation resulting from mutation of dyslexia candidate gene *Dcdc2*.

Key words: glutamate release, NMDA receptor, paired recording, presynaptic, reading disability

Introduction

Developmental dyslexia, or reading disability (RD), is a common learning disorder that is not understood at the level of neocortical microcircuits (Galaburda et al. 2006; Peterson and Pennington 2012; Rosenberg et al. 2012). While variants or mutations in any single gene do not cause dyslexia, genetic variants in *DCDC2* have been linked to an increased risk of dyslexia in multiple gene association studies across several populations (Meng et al. 2005; Schumacher et al. 2006; Couto et al. 2009; Marino et al. 2011, 2012). In addition, imaging-genetic studies have started to establish correlations between gray/white matter volume and *DCDC2* variants in brains regions implicated in reading, including superior prefrontal, temporal, and occipital networks (Meda et al. 2008; Darki et al. 2012; Jamadar et al. 2012; Eicher and Gruen 2013). Variants of *DCDC2* are also linked to functional activation and connectivity in human neocortex (Cope et al. 2012; Jamadar et al. 2012) as well as to performance in cognitive tasks, suggesting possible function in regulating structural and functional neural networks. Furthermore, mutation of *Dcdc2* in mice has been reported to lead to changes in learning and sensory processing. Consistent with a potential role of *DCDC2* in a subset of cognitive functions, *Dcdc2* mutant mice display deficits in performance of some, generally more difficult maze tasks, suggesting impaired visuo-spatial working memory (Gabel et al.

2011). Poorer performance by mutant mice in modified radial arm maze tasks further confirmed deficits in working memory as a result of *Dcdc2* mutation (Truong et al. 2014). In addition, prepulse inhibition paradigm revealed impaired rapid auditory processing in *Dcdc2* mutant mice (Truong et al. 2014), difficulties in which have also been found in up to 63% of RD individuals (Ramus 2003; Raschle et al. 2013). These studies provide compelling evidence that *Dcdc2* mutation results in neurological changes that underlie cognitive impairments, and yet little is known about these changes at the cellular, synaptic level when *Dcdc2* function is compromised.

Requirements of *Dcdc2* for normal electrophysiological patterns are beginning to be revealed by analyzing electrophysiological responses in *Dcdc2* mutant mice (Che et al. 2013). Specifically, neocortical pyramidal neurons in layers 2/3 and 4 in *Dcdc2* mutants display degraded spike-time precision caused by elevation in spontaneous NMDAR activation (Che et al. 2013). These results suggest that glutamatergic synaptic transmission might be abnormal in *Dcdc2* mutant mice, and led us to further investigate synaptic changes caused by *Dcdc2* mutation. We report in this study that the probability of excitatory transmitter release is elevated in layer 4 neurons in somatosensory neocortex of *Dcdc2* mutants. Using pharmacological approaches and paired whole-cell recordings, we showed that the elevated release is mediated by increased NMDAR activation on the presynaptic neuron, and is present between layer 4–layer 4 connections but not thalamocortical inputs. The link between *Dcdc2* gene function and elevated transmitter release mediated by NMDAR activation discovered here may indicate novel therapeutic targets, particularly for forms of RD that are nonresponsive to current interventions.

Materials and Methods

Immunohistochemistry and Microscopy

All experiments involving animals were performed under the approval of the University of Connecticut Animal Care and Use Committee. For histology, P25 Tg(Dcdc2a-EGFP)JC 158 Gsat mice were transcardially perfused under deep anesthesia with 4% paraformaldehyde in 1X phosphate-buffered saline. Brains were postfixed for 24 h prior to being sectioned with a vibratome (Leica) at 60 µm, and processed for immunostaining as floating sections. Primary antibody used was goat anti-GFP (1:1000, Molecular Probes) and secondary antibody was rabbit anti-goat conjugated with Alexa 488 (1:400, Molecular Probes). Photomicrographs were acquired with Zeiss Axio Imager 2 with a Zeiss ApoTome module.

Acute Brain Slice Preparation

P20-P28 wild-type and *Dcdc2* mutant mice were deeply anesthetized with isoflurane and then decapitated. Brains were rapidly removed and immersed in ice-cold oxygenated (95% O_2 and 5% CO_2) dissection buffer containing (in mM): 83 NaCl, 2.5 KCl, 1 NaH_2PO_4, 26.2 $NaHCO_3$, 22 glucose, 72 sucrose, 0.5 $CaCl_2$, and 3.3 $MgCl_2$. Coronal slices (400 µm) were cut using a vibratome (VT1200S, Leica), incubated in dissection buffer for 40 min at 34°C, and then stored at room temperature for reminder of the recording day. All slice recordings were performed at 34°C unless otherwise specified. Slices were visualized using IR differential interference microscopy (E600FN, Nikon) and a CCD camera (QICAM, QImaging). Individual cells were visualized with a ×40 Nikon Fluor water immersion (0.8 NA) objective.

Whole-Cell Recording

For all experiments, external recording buffer was oxygenated (95% O_2 and 5% CO_2) and contained (in mM): 125 NaCl, 25 $NaHCO_3$, 1.25 NaH_2PO_4, 3 KCl, 25 dextrose, 1 $MgCl_2$, and 2 $CaCl_2$. Patch pipettes were fabricated from borosilicate glass (N51A, King Precision Glass, Inc.) to a measured tip resistance of 2–5 MΩ when pipettes were filled with an internal solution containing (in mM): 125 potassium gluconate, 10 KCl, 10 HEPES, 4 Mg-ATP, 0.3 Na-GTP, 0.1 EGTA, 10 phosphocreatine, 0.05% biocytin, adjusted to pH 7.3 with KOH and to 278 mOsm with double-distilled H_2O. Signals were amplified with a Multiclamp 700A amplifier (Molecular Devices), digitized with an ITC-18 digitizer (HEKA Instruments, Inc.), and filtered at 2 KHz. Data were monitored, acquired, and in some cases analyzed using Axograph X software. Series resistance was monitored throughout the experiments by applying a small test voltage step and measuring the capacitive current. Series resistance was 5–25 MΩ and only cells with <20% change in series resistance and holding current were included for analysis. Liquid junction potential was not corrected.

All miniature excitatory postsynaptic currents (mEPSCs) were measured in the presence of the $GABA_A$ receptor blocker SR-95531 (Gabazine, 5 µM, Ascent Scientific) and in tetrodotoxin (TTX, 1 µM, Ascent Scientific) to isolate α-amino-3-hydroxy-5-methyl-4-isoxazolepropionic acid receptor (AMPAR)-mediated events. AMPAR-mediated mEPSC were recorded at −80 mV and MK-801 (1 mM) was added in recording pipette additionally to block the postsynaptic NMDAR-mediated currents in experiments where the effect of NMAR blockade in presynaptic cells was examined. Frequency, amplitude, rise, and decay time of mEPSCs were measured before and after the application of the NMDAR blocker DL-2-amino-5-phosphopentanoic acid (DL-APV, also abbreviated as APV, 100 µM, Ascent Scientific). 100 µM DL-APV washes were 8–10 min in duration and 180 s chart recordings before and after (while APV application continued) the drug wash were acquired and used for analysis. In specified experiments, Ro25-6981 (0.5 µM, Ascent Scientific) was used to block NR2B subunits; *N*-methyl-D-aspartic acid (NMDA, 20 µM, Tocris) or threo-β-benzyloxyaspartic acid (TBOA, 30 µM, Tocris) was used to increase glutamate receptor activation. To detect mEPSC events, a variable amplitude template was slid through the 180 s chart recordings (Clements 1997). The parameters of the template, including amplitude, 10–90% rise time, and decay time, were determined based on an average of real events as well as previously reported values. The detection threshold was 3–7 times of the noise standard deviation, and events with large baseline error were rejected additionally.

Evoked postsynaptic currents (EPSCs) were evoked using an isolated pulse stimulator unit (A-M system, model 2100, Sequim, WA, USA) with a glass electrode filled with the same external recording solution, placed 100–150 µm lateral to the recording pipette for extracellular stimulation of horizontal layer 4 connections. For paired-pulse experiments pairs of stimuli (30 and 50 Hz for experiment in Fig. 1) were delivered every 20 s and EPSCs were recorded at −80 mV to isolate AMPAR-mediated excitatory responses. In experiments where the effect of APV was accessed, MK-801 (1 mM) was added in recording pipette to ensure blockade of postsynaptic NMDAR-mediated currents. Small adjustments were made to the placement of the stimulating electrode so that single-peak EPSC responses were elicited. In cases where consistent single-peak EPSCs were unachievable, only the first, well-defined peak of the multicomponent EPSCs were used for analysis. Amplitude of the EPSCs was measured relative to a 2-ms baseline period 1 ms before the onset of the stimulation. For thalamocortical stimulation, slices were prepared following methods described by Agmon and Connors (1991) with

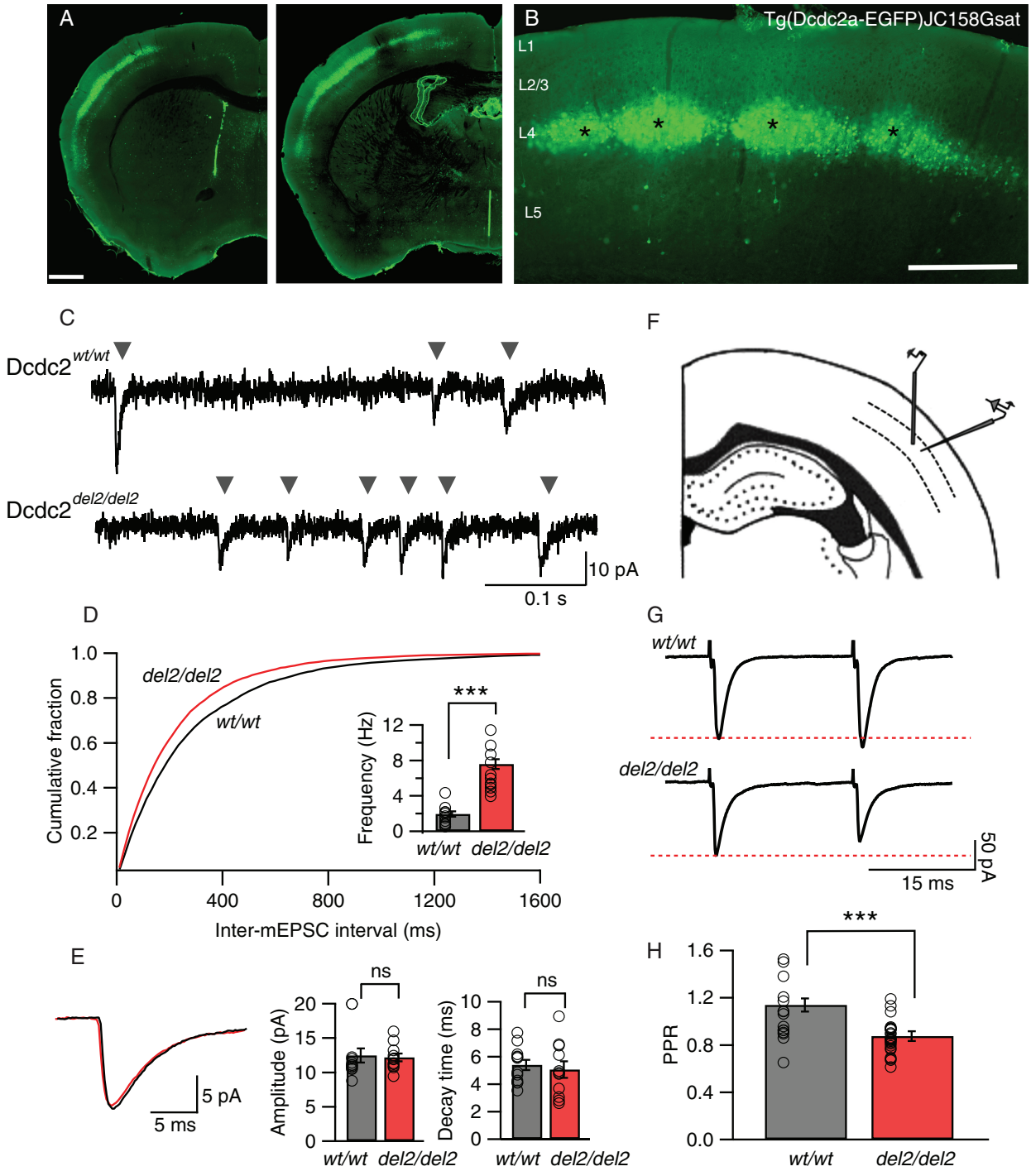

Figure 1. Somatosensory layer 4 neurons in Dcdc2$^{del2/del2}$ mice show increased glutamatergic synaptic activity. (*A*) Cells labeled by a BAC GFP transgene in the Dcdc2-EGFP GENSAT mouse [Tg(Dcdc2a-EGFP)JC158Gsat] are primarily within layer 4 of neocortex. (*B*) Somatosensory neocortex contains the highest density of GFP-positive neurons. Cortical layers 1–5 are labeled. Asterisks indicate sample barrels. Scale bars: *A*: 500 µm, *B*: 100 µm. (*C*) Sample traces of AMPAR-mediated mEPSCs from a Dcdc2$^{wt/wt}$ (top) and a Dcdc2$^{del2/del2}$ (bottom). Gray arrowheads indicate individual events. (*D*) Cumulative probability histogram for inter-mEPSC interval for Dcdc2$^{wt/wt}$ and Dcdc2$^{del2/del2}$ neurons. The histogram is from 11 recorded cells in Dcdc2$^{del2/del2}$ and 12 cells in Dcdc2$^{wt/wt}$ layer 4 somatosensory cortex. Kolmogorov–Smirnov test, $P < 0.05$. Inset, mean mEPSC frequency for Dcdc2$^{wt/wt}$ and Dcdc2$^{del2/del2}$ neurons ($P < 0.0001$). (*E*) Average mEPSC waveforms (Dcdc2$^{wt/wt}$: black, Dcdc2$^{del2/del2}$: red), mean amplitude ($P = 0.83$) and decay time ($P = 0.63$) for Dcdc2$^{del2/del2}$ and Dcdc2$^{wt/wt}$. Student's *t*-test, Dcdc2$^{wt/wt}$: $n = 12$, Dcdc2$^{del2/del2}$: $n = 11$. (*F*) Schematic of the somatosensory cortical slice and approximate placements of recording and stimulating electrodes. (*G*) Representative synaptic responses in paired-pulse stimulation experiments in a Dcdc2$^{wt/wt}$ and a Dcdc2$^{del2/del2}$ layer 4 neuron. Red-dotted line indicates the level of the first synaptic response in each pair. (*H*) Bar graph showing paired-pulse ratios (PPR, second response amplitude/first response amplitude) for recordings within layer 4 of Dcdc2$^{del2/del2}$ and Dcdc2$^{wt/wt}$ neocortex ($P = 0.001$). Student's *t*-test; Dcdc2$^{wt/wt}$: $n = 15$, Dcdc2$^{del2/del2}$: $n = 27$. Open circles indicating individual neurons. ***$P < 0.001$; ns, $P > 0.05$.

modifications (Porter et al. 2001). The stimulating electrode was placed in the ventrobasal nucleus of the thalamus, and recordings were made at room temperature in excitatory cells in the barrel cortex. To compare the effect of APV on first-spike amplitude and variance, baclofen (5 μM), a $GABA_B$ receptor agonist, was used to reduce presynaptic release, and NBQX (0.3 μM) was used to partially block postsynaptic AMPARs. For every cell recorded, 20–50 sweeps were collected after each drug wash.

For recording synaptically connected pairs of layer 4 neurons, simultaneous whole-cell recordings were performed on 2 cells located in close proximity. Synaptic connections were established by eliciting action potentials in one neuron by injecting 3 nA current for 1 ms, and recording EPSCs from another. Resting membrane potential (RMP) of the presynaptic neuron was adjusted to −75 mV with holding current, and ESPCs were recorded in the postsynaptic cell at −80 mV. Of 64 pairs attempted in wild types, 14 pairs were synaptically coupled (connectivity rate: 21.9%), similar to previous reports (Feldmeyer et al. 1999; Brasier and Feldman 2008). Four of the 14 pairs were not used for analysis due to one of the cells in the pair either loosing a tight seal recording or a large change in series resistance before completing all protocols. In *Dcdc2* mutants, 69 pairs were attempted and 16 pairs were found synaptically coupled (connectivity rate: 23.2%). Three of the 16 pairs were excluded from data analysis due to one of the cells in the pair either loosing a tight seal recording or developing a large increase in series resistance before completing all protocols. Pairs found to be synaptically coupled were tested for bidirection connections, of which none of the 14 wild-type pairs were connected bidirectionally, and 3 of the 16 mutant pairs were. In these 3 mutant pairs, the stronger synaptic connection was used for analysis. Once a synaptic connection was identified, pairs of action potentials were generated in the presynaptic cell at 30 Hz every 20 s, and unitary EPSCs were recorded in the postsynaptic cell. For every cell recorded, 50 sweeps were collected after each drug wash condition. Paired-pulse ratios and response amplitudes were determined for each pair then averaged, excluding failures.

For NMDA-to-AMPA ratio experiments, the internal solution contained (in mM): 110 $CsMeSO_4$, 10 CsCl, 10 HEPES, 10 Cs_4-BAPTA, 5 QX-314·Br, 0.1 spermine, 4 Mg-ATP, 0.4 Na-ATP, 10 phosphocreatine, 0.05% biocytin, adjusted to pH 7.3 with CsOH and to 278 mOsm with double-distilled H_2O. Recordings began at least 10 min after initial whole-cell recording was achieved to allow dialysis of Cs^+ internal solution. A single extracellular stimulation was delivered every 10 s, while the cell was held at either −90 mV (AMPAR-mediated responses), 0 mV, or +50 mV (mixed AMPAR-mediated and NMDAR-mediated responses). Amplitudes of AMPAR-mediated current were measured as the average amplitude of a 1-ms window at the response peak relative to the baseline when the cell was clamped at −90 mV. The NMDAR-mediated current was measured at +50 mV as the average of a 10-ms window beginning 25 ms after the stimulus artifact, when AMPAR-mediated current has decayed to baseline (modified from Myme and Sugino (2003)). For measuring spontaneous NMDAR-mediated events, cells were voltage clamped at +40 mV, and the AMPAR antagonist NBQX (10 μM) was included in addition to SR-95531 and TTX in the external recording buffer. Evident detection methods, similar to those described for mEPSC measurement but with different parameters, were used to obtain the average waveforms, amplitude, rise, and decay time.

Data Analysis and Statistics

Data analysis was performed using Axograph X built-in analysis and IGOR Pro software (Wavemetrics) on a Macintosh computer. Statistics were performed using Prism 6 software (Graphpad), and graphs were generated in IGOR Pro software. Statistical significance was determined using either Student's *t*-tests (indicated on graphs with asterisks, $^*P < 0.05$; $^{**}P < 0.01$; $^{***}P < 0.001$; ns, $P > 0.05$) or ANOVA (indicated by *P* values in legends as well as results). For multiple comparisons tests following ANOVA, multiplicity adjusted *P* values were reported (indicated on graphs with asterisks, $^*P < 0.05$; $^{**}P < 0.01$; $^{***}P < 0.001$; ns, $P > 0.05$). Significance was based on *P* values <0.05. Means and standard errors were reported for all results unless otherwise specified.

Results

Glutamatergic Synaptic Activity in Layer 4 Is Elevated Following *Dcdc2* Mutation

We made recordings from Layer 4 regular spiking neurons in somatosensory neocortex of the mouse both because these neurons showed the strongest *Dcdc2* promoter activity as seen by dense eGFP labeling in *Dcdc2*-BAC transgenic mice (Fig. 1*A*,*B*; GENSAT BAC transgene, Tg(Dcdc2a-EGFP)JC158Gsat), and because previous in situ hybridization results showed that *Dcdc2*, while expressed at some level throughout the brain, shows expression in neocortex (Meng et al. 2005; Magdaleno et al. 2006; Burbridge et al. 2008). To test for changes in synaptic properties in layer 4 neocortical neurons, we first compared the frequency and amplitude of mEPSCs in wild-type ($Dcdc2^{wt/wt}$, or *wt/wt* in figures) and *Dcdc2* mutant mice ($Dcdc2^{del2/del2}$, or *del2/del2* in figures). Spontaneous glutamatergic synaptic currents were significantly elevated in frequency in the mutants (1.93 ± 0.31 Hz in $Dcdc2^{wt/wt}$ vs. 7.66 ± 0.87 Hz in $Dcdc2^{wt/wt}$, $t_{21} = 6.39$, $P < 0.0001$, Fig. 1*C*,*D*), but were unchanged in amplitude (12.46 ± 1.04 pA in $Dcdc2^{wt/wt}$ vs. 12.19 ± 0.56 pA in $Dcdc2^{del2/del2}$, $t_{21} = 0.22$, $P = 0.83$) or decay (5.40 ± 0.38 ms in $Dcdc2^{wt/wt}$ vs. 5.06 ± 0.60 ms in $Dcdc2^{del2/del2}$, $t_{21} = 0.48$, $P = 0.63$) (Fig. 1*E*) relative to $Dcdc2^{wt/wt}$ controls. An increase in the frequency of glutamatergic mEPSCs, without change in amplitude or decay, points to either changes in probability of neurotransmitter release, or an increase in the number of synapses.

We next tested whether there was an increase in the probability of transmitter release by performing paired-pulse analysis on electrically EPSCs by stimulation within layer 4, 50–100 μm lateral to the recorded layer 4 neurons (Fig. 1*F*,*G*). All evoked responses were measured in the presence of SR-95531 (gabazine, 5 μM) to isolate excitatory synaptic circuitry from inhibitory circuits. The amplitude of the second excitatory synaptic response in wild-type neurons was either the same or slightly elevated relative to the first response amplitude (Fig. 1*G*,*H*). In contrast, the mutants consistently showed paired-pulse depression, suggesting a higher probability of transmitter release (Del Castillo and Katz 1954; Zucker and Regehr 2002). Paired-pulse ratio was significantly lower in the mutants relative to wild types (1.08 ± 0.06 in $Dcdc2^{wt/wt}$ vs. 0.86 ± 0.02 pA in $Dcdc2^{del2/del2}$, $t_{40} = 3.55$, $P = 0.001$, Fig. 1*H*), and this observation, along with the increase in spontaneous synaptic frequency without a change in spontaneous event amplitude or decay, is consistent with elevation in the presynaptic probability of transmitter release in Dcdc2 mutants.

Elevated mEPSC Frequency in *Dcdc2* Mutants Is Decreased by NMDAR Antagonists

Presynaptic transmitter release can be influenced by activation of several types of metabotropic receptors (Takahashi and Kajikawa 1998; Cartmell and Schoepp 2000; Karim et al. 2001; Kreitzer et al. 2002; Freund et al. 2003) and ligand-gated ion channels (Berretta

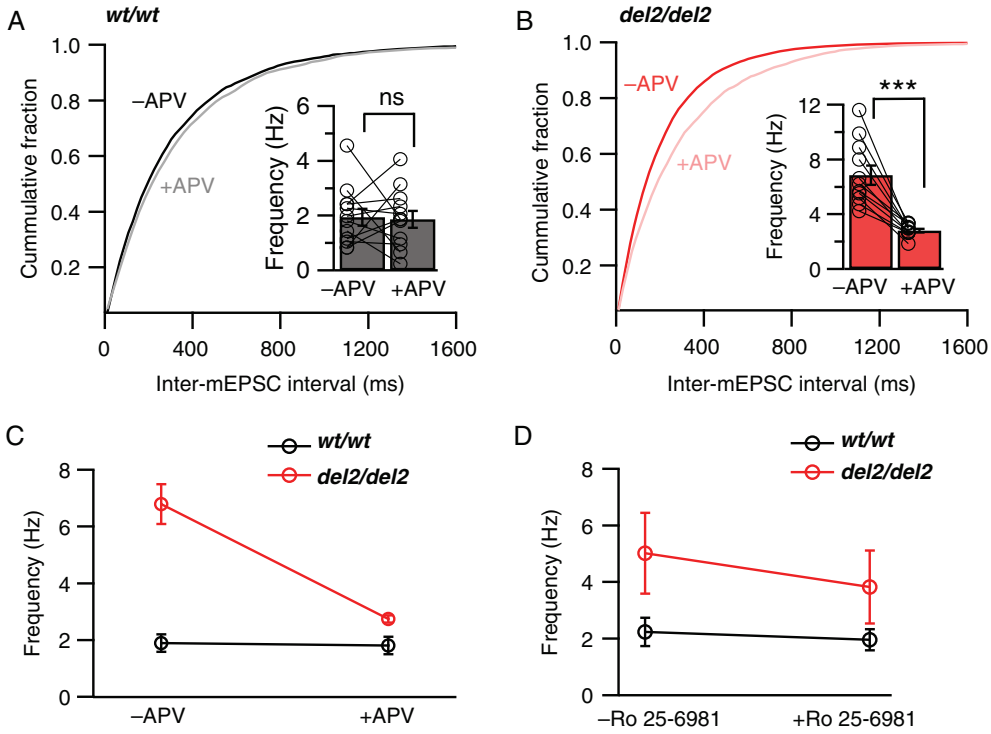

Figure 2. Blockade of NMDARs decreases elevated spontaneous vesicle release in Dcdc2$^{del2/del2}$ mice. Cumulative probability histograms showing intervals between mEPSCs in (*A*) Dcdc2$^{wt/wt}$ (black) and (*B*) Dcdc2$^{del2/del2}$ (red) layer 4 excitatory neurons before and after the application of DL-APV (100 µM). Kolmogorov–Smirnov test, –APV versus +APV, Dcdc2$^{wt/wt}$: $P > 0.05$; Dcdc2$^{del2/del2}$: $P < 0.05$. Inset, mean mEPSC frequencies for Dcdc2$^{wt/wt}$ and Dcdc2$^{del2/del2}$ neurons. Open circles indicate individual neurons. (*C*) Interaction graph showing the differential effect of APV on mEPSC frequencies in Dcdc2$^{del2/del2}$ and Dcdc2$^{wt/wt}$ neurons. Repeated-measures ANOVA, genotype×APV application interaction: $F_{1,21} = 27.21$, $P < 0.0001$. Followed by Bonferroni's multiple comparisons test within genotype (significance indicated on insets in *A* and *B*): Dcdc2$^{wt/wt}$: $P > 0.05$, Dcdc2$^{del2/del2}$: $P < 0.0001$; between genotype: –APV: $P < 0.0001$, +APV: $P > 0.05$; Dcdc2$^{wt/wt}$: $n = 12$, Dcdc2$^{del2/del2}$: $n = 11$. TTX (1 µM) and SR-95531 (5 µM) were included in the extracellular recording buffer, and MK-801 (1 mM) internally to block postsynaptic NMDARs. (*D*) Interaction graph showing the differential effect of Ro 25–6981 (0.5 µM) on mEPSC frequencies in Dcdc2$^{del2/del2}$ versus Dcdc2$^{wt/wt}$ cells. Repeated-measures ANOVA, genotype×Ro 25-6981 application interaction: $F_{1,18} = 4.68$, $P < 0.05$. Dcdc2$^{wt/wt}$: $n = 10$, Dcdc2$^{del2/del2}$: $n = 10$. ***$P < 0.001$; ns, $P > 0.05$.

and Jones 1996; Chittajallu et al. 1996; Turecek and Trussell 2001). Several studies have recently shown that activation of NMDARs can increase release probability in multiple brain regions including the neocortex (Corlew et al. 2008; McGuinness et al. 2010; Larsen et al. 2011; Kunz et al. 2013). We therefore tested the possibility that the increased probability of release in Dcdc2$^{del2/del2}$ mice may be due to increased activation of NMDARs. We specifically blocked postsynaptic NMDARs in the recorded cells by a combination of hyperpolarization (–80 mV) and intracellular injection of MK-801 through the recording pipette (1 mM, in recording pipette). In these conditions, we found that bath application of the NMDAR antagonist APV (DL-APV, 100 µM) significantly decreased the frequency of mEPSCs in the mutant neurons, returning frequency of synaptic events back to wild-type levels (repeated-measures ANOVA, $F_{1,21} = 27.21$, $P < 0.0001$, Bonferroni's multiple comparisons tests see figure legend, Fig. 2*A*–*C*). We also tested the NR2B subunit-specific blocker Ro 25–6981 (0.5 µM), and found that blocking NR2B subunit-containing NMDARs also significantly reduced mEPSC frequency in the mutants (repeated-measures ANOVA, $F_{1,18} = 4.68$, $P = 0.042$, Fig. 2*D*).

Increased mEPSC Frequencies in *Dcdc2* Mutants Is Not Caused by Elevated Ambient Glutamate

One possibility for elevated activation of NMDARs causing increased synaptic release of glutamate would be if ambient glutamate levels were elevated and this caused an increased baseline activation of NMDARs acting presynaptically. Elevations in extracellular glutamate concentrations without changes in receptor number or function could then lead to NMDAR-dependent increases in mEPSC frequencies. To test this, we measured mEPSC frequencies in high concentrations of the NMDAR agonist NMDA (20 µM) or in the presence of the excitatory amino acid transporters blocker TBOA (30 µM), followed by bath application of APV in both *Dcdc2* mutants and wild types. If the elevated mEPSC frequency in mutants were the result of high concentrations of ambient glutamate alone, we reasoned that mEPSC frequency in wild types would be increased to mutant levels, and this would be blockable by APV. We found, in contrast, that mEPSC frequencies in wild types did not increase to mutant levels in the presence of NMDA or TBOA, and that addition of APV did not affect wild-type mEPSC frequencies (repeated-measures ANOVA, NMDA: $F_{2,30} = 2.60$; TOBA: $F_{2,22} = 2.41$, Tukey's pairwise multiple comparisons tests, see figure legend, Fig. 3*A*,*B*). Elevated ambient agonist activation of NMDARs is therefore not sufficient to explain the increased frequency of spontaneous glutamatergic synaptic events in *Dcdc2* mutants.

We also considered the possibility that depolarized RMP (Che et al. 2013) could lead to increased spontaneous synaptic glutamate release. To test this, we altered external K^+ concentration in the recording solution. We did not, however, observe an increase in wild-type mEPSC frequencies that reached mutant levels when extracellular K^+ concentration was elevated from 3 to 6 mM (2.55 ± 0.58 vs. 2.75 ± 0.60 Hz, $t_5 = 0.97$, $P = 0.37$) to achieve depolarization comparable with mutant levels (–73.80 ± 1.00 to –62.90 ± 2.40 mV), and APV did not decrease mEPSC frequencies

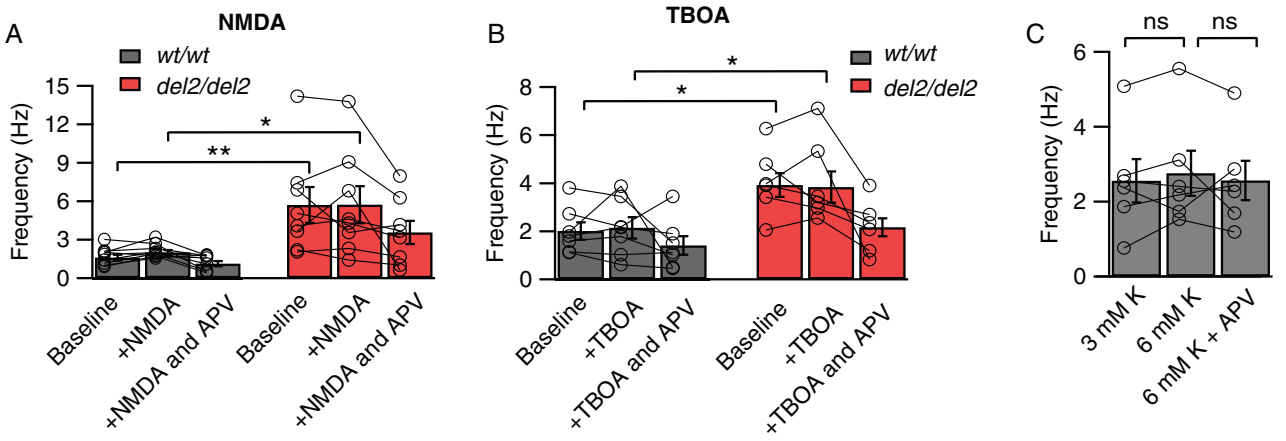

Figure 3. Elevated mEPSC frequency in Dcdc2$^{del2/del2}$ is not caused by changes in ambient glutamate level or difference in RMP. (*A*) Average mEPSC frequencies during baseline, NMDA (20 μM), NMDA (20 μM) plus DL-APV (100 μM) application for Dcdc2$^{wt/wt}$ (gray bars) and Dcdc2$^{del2/del2}$ (red bars) layer 4 neurons. Repeated-measures ANOVA (between variables: genotype, within variables: drug application), main effect of genotype on frequency: $F_{1,15} = 9.14$, $P < 0.01$. Followed by Tukey's multiple comparisons tests, difference significant between Dcdc2$^{wt/wt}$ versus Dcdc2$^{del2/del2}$: baseline ($P < 0.01$), +NMDA ($P < 0.05$); no significance: +NMDA and APV ($P = 0.14$). Dcdc2$^{wt/wt}$: $n = 9$, Dcdc2$^{del2/del2}$: $n = 8$. (*B*) Average mEPSC frequencies during baseline, TBOA (30 μM), TBOA (30 μM) plus DL-APV (100 μM) application for Dcdc2$^{wt/wt}$ (gray bars) and Dcdc2$^{del2/del2}$ (red bars) layer 4 neurons. Repeated-measures ANOVA, main effect of genotype on frequency: $F_{1,11} = 7.27$, $P < 0.05$. Followed by Tukey's multiple comparisons tests, difference significant between Dcdc2$^{wt/wt}$ versus Dcdc2$^{del2/del2}$: baseline ($P < 0.05$), +TBOA ($P < 0.05$); no significance: +TBOA and APV ($P = 0.64$). Dcdc2$^{wt/wt}$: $n = 7$, Dcdc2$^{del2/del2}$: $n = 6$. (*C*) Average mEPSC frequencies for Dcdc2$^{wt/wt}$ neurons in 3 mM K^+ (normal), 6 mM K^+ and 6 mM K^+ plus APV. One-way ANOVA with Tukey's multiple comparisons tests, $F_{1.42,7.08} = 0.34$, $P = 0.65$, $n = 6$. Open circles connected with lines indicate individual neurons. *$P < 0.05$; **$P < 0.01$; ns, $P > 0.05$.

in wild-type neurons with K^+-depolarized membrane potentials (One-way ANOVA with Tukey's multiple comparisons tests, $F_{1.42,7.08} = 0.34$, $P = 0.65$, Fig. 3*C*). These results indicate that elevated RMP is not sufficient to increase spontaneous glutamatergic synaptic events to levels apparent in *Dcdc2* mutants.

Evoked Glutamatergic Synaptic Transmission Is Enhanced in *Dcdc2* Mutants due to Increased NMDAR Activity

We next tested whether the increase in probability of release during electrically evoked neurotransmission was dependent on NMDAR activation. To do this, we measured paired-pulse ratios to electrically evoked synaptic responses in wild types and mutants before and after APV bath application. As above, MK-801 was included in the recording pipette to block NMDARs in the postsynaptic cell. Bath application of APV in wild-type slices had no significant effect on paired-pulse ratios of synaptic responses (1.14 ± 0.05 before APV vs. 1.12 ± 0.08 in APV, $t_7 = 0.22$, $P = 0.83$, Fig. 4*A*,*B*), while in mutants APV significantly increased paired-pulse ratios (0.85 ± 0.04 before APV vs. 1.02 ± 0.05 in APV, $t_9 = 4.76$, $P = 0.001$, Fig. 4*B*), reverting them to levels observed at wild-type synapses (repeated-measures ANOVA, $F_{1,16} = 5.05$, $P = 0.039$, Bonferroni's multiple comparisons tests, see legend, Fig. 4*C*). In addition, APV decreased the amplitude of the first synaptic response in mutants (normalized, 1.06 ± 0.02 before APV and 0.71 ± 0.05 in APV, $t_7 = 7.08$, $P = 0.0002$) but not wild types (0.96 ± 0.02 before APV and 0.98 ± 0.03 in APV, $t_6 = 1.11$, $P = 0.31$, Fig. 4*D*,*E*), indicating further an enhancement in evoked synaptic responses in *Dcdc2* mutants dependent on presynaptic NMDAR activation. Taken together, these results suggest that similar to its effect on spontaneous release, elevated NMDAR activity on presynaptic cells is necessary to increased evoked transmitter release in mutant layer 4 neurons.

In order to further assess whether the effect of NMDAR block on *Dcdc2* mutants was through presynaptic mechanisms, we determined the relationship between the coefficient of variation (CV) in synaptic responses, $1/CV^2$, and the normalized response amplitudes before and after the application of APV (Fig. 4*F*). In this method, a data point falling under the diagonal line on the plot suggests presynaptic changes, since smaller response amplitude as a result of decreased transmitter release is accompanied by greater decrease in variation (Malinow and Tsien 1990; Faber and Korn 1991). In mutant neurons, APV decreased the amplitude of synaptic responses and this was paralleled by a reduction in $1/CV^2$. A similar reduction was observed with baclofen (5 μM), a $GABA_B$ receptor agonist known to act presynaptically (Manabe et al. 1993; Tzounopoulos et al. 2007). In contrast, subsaturating concentration of NBQX (0.3 μM), which reduces response amplitude by blocking postsynaptic AMPA receptors, left CV unaffected (Fig. 4*F*). These results further support that in *Dcdc2* mutants, NMDAR activation alters evoked release by presynaptic mechanisms.

Evidence for a presynaptic locus of NMDAR-mediated change was further strengthened by a set of negative results assessing postsynaptic NMDAR function and expression by measuring the NMDAR/AMPAR ratio ((Myme and Sugino 2003), Fig. 5*A*,*B*), the waveform of spontaneous postsynaptic NMDAR-mediated events (Fig. 5*C*,*D*), and the expression of NR2B at post synaptic densities. We found no significant differences relative to wild type in NMDAR/AMPAR ratios of EPSCs (1.11 ± 0.24 in Dcdc2$^{wt/wt}$ vs. 1.18 ± 0.32 in Dcdc2$^{del2/del2}$, $t_{14} = 0.18$, $P = 0.86$, Fig. 5*B*) or in amplitudes of spontaneous miniature NMDAR-mediated synaptic events recorded at +40 mV (8.76 ± 0.75 in Dcdc2$^{wt/wt}$ vs. 10.69 ± 0.86 in Dcdc2$^{del2/del2}$, $t_{22} = 0.14$, $P = 0.14$, Fig. 5*D*), despite the increase in their frequency reported previously (Che et al. 2013). In addition, NR2B protein levels at the postsynaptic densities (PSDs) remained unaltered in the mutants by western blot analysis (0.59 ± 0.15 in Dcdc2$^{wt/wt}$ vs. 0.66 ± 0.20 in Dcdc2$^{del2/del2}$, relative to beta-actin, $t_6 = 0.25$, $P = 0.81$, Supplementary Fig. 2). These results together suggest that postsynaptic NMDAR function is not directly altered in *Dcdc2* mutants.

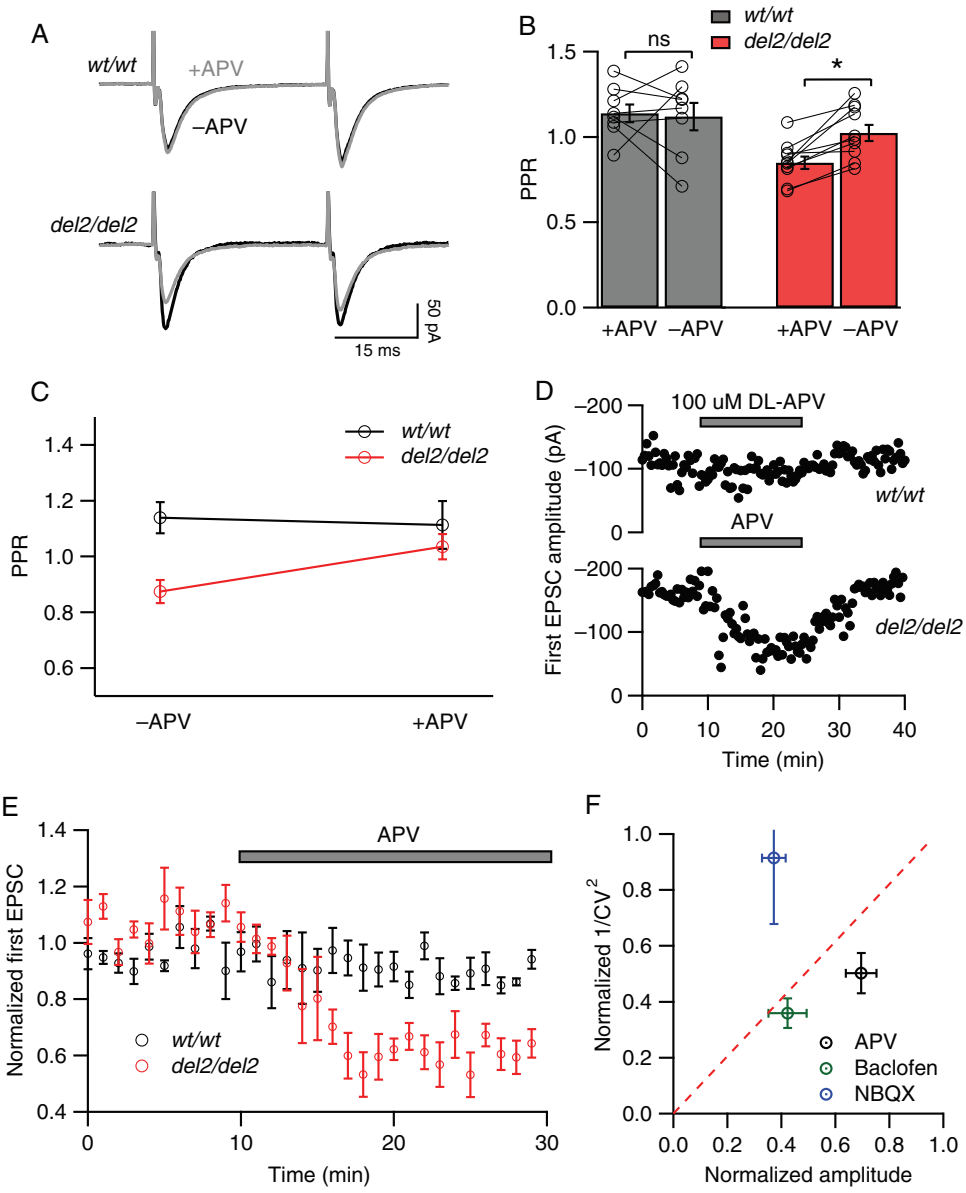

Figure 4. Blockade of NMDARs reduces probability of evoked release in Dcdc2$^{del2/del2}$ but not Dcdc2$^{wt/wt}$ mice. (*A*) Representative paired-pulse responses elicited by extrasynaptic electrical stimulation in a Dcdc2$^{wt/wt}$ (top) and Dcdc2$^{del2/del2}$ (bottom) layer 4 excitatory cell before (black) and after (gray) APV application. (*B*) Effects of APV application on PPR in Dcdc2$^{wt/wt}$ (gray bars) and Dcdc2$^{del2/del2}$ (red bars) neurons. Open circles connected with lines indicate individual neurons. (*C*) Interaction graph showing the mean paired-pulse ratios for Dcdc2$^{wt/wt}$ and Dcdc2$^{del2/del2}$ neurons before and after APV. Repeated-measures ANOVA, genotype × APV application interaction: $F_{1,16} = 5.05$, $P < 0.05$. Followed by Bonferroni's multiple comparisons test within genotype (significance indicated in *B*): Dcdc2$^{wt/wt}$: adjusted $P > 0.05$; Dcdc2$^{del2/del2}$: $P < 0.05$). Dcdc2$^{wt/wt}$: $n = 8$, Dcdc2$^{del2/del2}$: $n = 10$. (*D*) Representative plot of peak amplitudes of the first AMPA-mediated EPSCs over time in a Dcdc2$^{wt/wt}$ (upper) and Dcdc2$^{del2/del2}$ (lower) layer IV neuron before, during, and after APV application. Pairs of stimulations were delivered every 20 s. (*E*) Averages of normalized first EPSC amplitudes in Dcdc2$^{wt/wt}$ ($n = 5$; black circles) and Dcdc2$^{del2/del2}$ ($n = 6$; red circles) neurons showing the absence of APV effect in Dcdc2$^{wt/wt}$ and decrease in amplitudes in Dcdc2$^{del2/del2}$ mice. Every 3 EPSCs were averaged (covering 1-min period), and normalized to the mean of the first minute. (*F*) CV analysis of Dcdc2$^{del2/del2}$ neurons by plotting EPSC amplitude ratio versus $1/CV^2$ ratio (postdrug/predrug) after and before NBQX (0.3 μM; blue circle, $n = 6$), baclofen (5 μM; green circle, $n = 4$), and DL-APV (100 μM; black circle, $n = 12$). Data points falling above the red-dotted line indicate a postsynaptic site of action, and those below a presynaptic site of action. *$P < 0.05$; ns, $P > 0.05$.

NMDAR-Mediated Increase in Presynaptic Glutamate Release at Layer 4–Layer 4 Connections but Not at Thalamocortical Connections

Layer 4 excitatory neurons in somatosensory barrel cortex mostly receive synaptic inputs from intracortical connections and from the thalamus (Benshalom and White 1986; Agmon and O'Dowd 1992; Feldmeyer et al. 1999; Petersen and Sakmann 2000; Schubert et al. 2003). Although the horizontal extracellular stimulation within layer 4 that we used in our experiments above should largely recruit intracortical connections as previously suggested (Feldman et al. 1998), given the high efficacy of thalamocortical synapses (Gil et al. 1999), it should be directly tested whether NMDAR-mediated change in release in *Dcdc2* mutants was present specifically at layer 4–layer 4 connections. We therefore isolated synaptic connections between layer 4 neurons by paired whole-cell recordings (Fig. 6A). Responses between

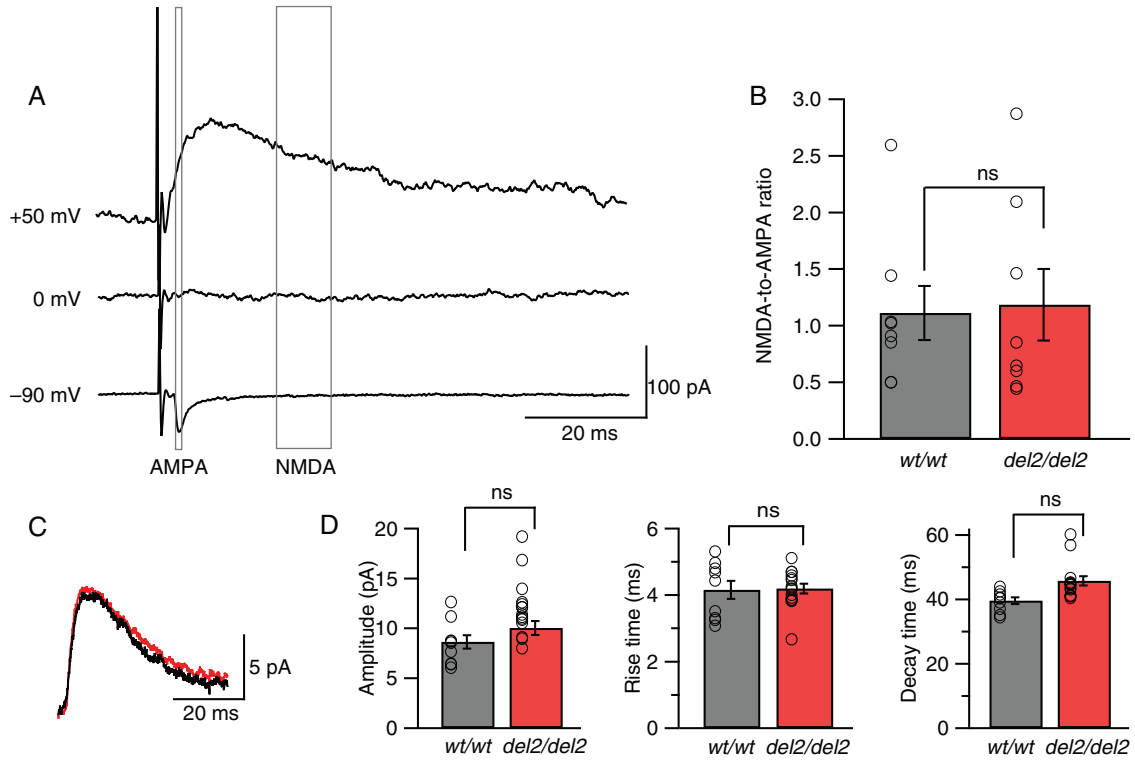

Figure 5. Postsynaptic NMDARs remain unaffected in Dcdc2$^{del2/del2}$ mice. (*A*) Averages of EPSCs evoked when a Dcdc2$^{wt/wt}$ layer 4 excitatory cell was held at −90, 0, and + 50 mV. Gray boxes indicate windows used to measure AMPAR-mediated component (1 ms at −90 mV) and NMDAR-mediated component (10 ms at +50 mV). (*B*) NMDA-to-AMPA ratios for Dcdc2$^{wt/wt}$ and Dcdc2$^{del2/del2}$ neurons ($t_{14} = 0.18$, $P = 0.85$). Open circles indicate individual neurons. Student's *t*-test. Dcdc2$^{wt/wt}$: $n = 8$, Dcdc2$^{del2/del2}$: $n = 8$. (*C*) Representative average waveforms of spontaneous miniature NMDAR-mediated synaptic events for a Dcdc2$^{wt/wt}$ (black) and a Dcdc2$^{del2/del2}$ (red) neuron. Membrane potential was held at +40 mV. Extracellular recording buffer included 10 µM NBQX, 5 µM SR-95531, and 1 µM TTX to isolate NMDAR-mediated events. (*D*) Mean amplitude ($t_{22} = 1.54$, $P = 0.14$), rise ($t_{22} = 0.13$, $P = 0.90$) and decay time ($t_{22} = 0.38$, $P = 0.71$) of average NMDA event waveforms. Open circles indicate individual neurons. Student's *t*-test. Dcdc2$^{wt/wt}$: $n = 9$, Dcdc2$^{del2/del2}$: $n = 15$. ns, $P > 0.05$.

layer 4 pairs were measured by eliciting single action potentials in the presynaptic neuron with RMPs adjusted to −75 mV, and recording EPSCs in the postsynaptic neuron at −80 mV in voltage clamp (Fig. 6A,E,F). Similar to results from extracellular stimulation, before applying NMDAR antagonists recordings from connected layer 4 pairs typically showed paired-pulse depression in *Dcdc2* mutants but paired-pulse facilitation in wild types, with a significant difference in their paired-pulse ratios (1.33 ± 0.16 in Dcdc2$^{wt/wt}$ vs. 0.83 ± 0.05 in Dcdc2$^{del2/del2}$, $t_{21} = 3.21$, $P = 0.0042$, Fig. 6B). In addition, we found both the CV of EPSC amplitudes (0.47 ± 0.05 pA in Dcdc2$^{wt/wt}$ vs. 0.29 ± 0.03 pA in Dcdc2$^{del2/del2}$, $t_{21} = 3.18$, $P = 0.0045$, Fig. 6C) and failure rate in mutant unitary connections to be significantly lower relative to wild-type ones (0.17 ± 0.04 in Dcdc2$^{wt/wt}$ vs. 0.06 ± 0.03 in Dcdc2$^{del2/del2}$, $t_{21} = 2.23$, $P = 0.037$, Fig. 6D), indicating higher probability of transmitter release. No significant difference in the average amplitude of unitary responses was found (16.24 ± 3.38 pA in Dcdc2$^{wt/wt}$ vs. 22.66 ± 3.42 pA in Dcdc2$^{del2/del2}$, $t_{21} = 1.31$, $P = 0.21$, data not shown).

To test whether NMDAR activity was responsible for the difference in transmission reliability between layer 4 neurons, we then bath applied APV and measured the effect of APV on presynaptic release probability. Consistent with extracellular stimulation experiments, APV had no significant effect on paired-pulse ratio (1.32 ± 0.16 before APV and 1.14 ± 0.13 in APV, $t_9 = 1.12$, $P = 0.29$, Fig. 6G) or response amplitude (16.24 ± 3.38 before APV and 14.58 ± 2.83 in APV, $t_9 = 1.36$, $P = 0.21$, Fig. 6J) in the wild types, whereas in Dcdc2 mutants, APV significantly increased paired-pulse ratio (0.83 ± 0.05 before APV and 1.04 ± 0.09 in APV, $t_{12} = 2.93$, $P = 0.01$, Fig. 6G), accompanied by a decrease in first response amplitude (22.66 ± 3.43 before APV and 17.60 ± 2.94 in APV, $t_{12} = 3.81$, $P = 0.003$, Fig. 6J). Notably, paired-pulse ratio was reverted back to wild-type levels in mutants by APV (repeated-measures ANOVA, $F_{1,21} = 5.45$, $P = 0.030$, Bonferroni's multiple comparisons tests, see legend, Fig. 6H), and 1/CV^2 versus amplitude analysis was consistent with the effect of APV on presynaptic release and not on postsynaptic response amplitudes (Fig. 6I).

We next tested whether thalamic inputs to layer 4 neurons were altered in mutants. In contrast to recordings from connected layer 4 pairs, we found paired-pulse ratios (Hull et al. 2009) that did not significantly differ between wild types and mutants (0.71 ± 0.05 in Dcdc2$^{wt/wt}$ vs. 0.68 ± 0.08 in Dcdc2$^{del2/del2}$). Moreover, APV had no significant effects on paired-pulse ratios (repeated-measures ANOVA, $F_{1,12} = 3.97$, $P = 0.070$, Bonferroni's multiple comparisons tests, see figure legend, Fig. 6K) or response amplitudes (first response amplitude, normalized, 1.02 ± 0.07 in Dcdc2$^{wt/wt}$ vs. 0.95 ± 0.07 in Dcdc2$^{del2/del2}$, $t_{12} = 0.72$, $P = 0.48$, Fig. 6L). In summary, these data suggest increased synaptically evoked release probability in *Dcdc2* mutants is mediated by enhanced activation specifically between L4-L4 connections.

Effect of NMDAR Activation in Mutants Is Enhanced by Elevated Evoked Glutamate

During paired recording experiments between layer 4 neurons, we observed greater increases in paired-pulse ratios after APV application in *Dcdc2* mutant neurons with larger response amplitudes.

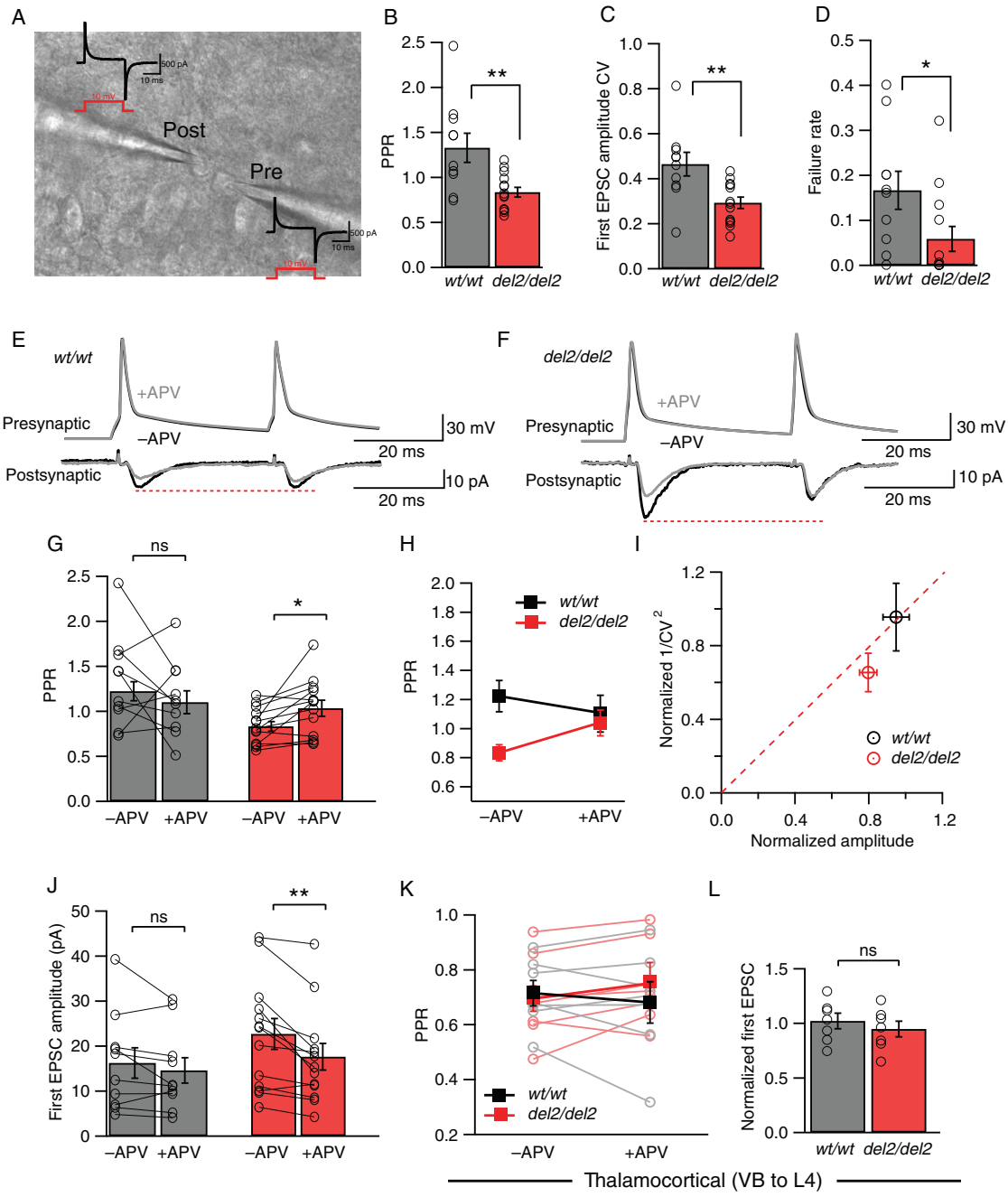

Figure 6. NMDAR-mediated increase in release probability is present at Dcdc2$^{del2/del2}$ layer 4-layer 4 excitatory synapses but not thalamocortical synapses. (*A*) Differential interference contrast image of example synaptically connected Dcdc2$^{wt/wt}$ layer 4 excitatory neurons. Current transients (black) responding to 10-mV test pulse (red) for these cells are displayed to demonstrate whole-cell configuration achieved. (*B*) Average PPRs ($P < 0.05$), (*C*) coefficient of variance (CV) of first response amplitudes ($P < 0.01$), and (*D*) failure rates ($P < 0.01$) of Dcdc2$^{wt/wt}$ and Dcdc2$^{del2/del2}$ responses. Student's *t*-test; Dcdc2$^{wt/wt}$: $n = 10$ pairs, Dcdc2$^{del2/del2}$: $n = 13$ pairs. Open circles indicate averages from individual neurons. Postsynaptic unitary EPSCs elicited by a pair of presynaptic action potentials in a (*E*) Dcdc2$^{wt/wt}$ and a (*F*) Dcdc2$^{del2/del2}$ layer 4 excitatory cell pair before (black) and after (gray) APV application. Dcdc2$^{wt/wt}$ traces correspond to pre- and postsynaptic neurons labeled in *A*. (*G*) Effects of APV application on PPR in Dcdc2$^{wt/wt}$ (gray bars) and Dcdc2$^{del2/del2}$ (red bars) neurons. Student's *t*-test, Dcdc2$^{wt/wt}$: $t_9 = 1.12$, $P = 0.29$; Dcdc2$^{del2/del2}$: $t_{12} = 2.93$, $P = 0.01$. Open circles connected with lines indicate individual neurons. (*H*) Interaction graph showing the mean PPR for Dcdc2$^{wt/wt}$ (black filled square) and Dcdc2$^{del2/del2}$ (red filled square) cells before and after APV. Repeated-measures ANOVA, genotype × APV application interaction: $F_{1,21} = 5.45$, $P < 0.05$. Followed by Bonferroni's multiple comparisons test, difference significant between Dcdc2$^{wt/wt}$ versus Dcdc2$^{del2/del2}$ before APV ($P < 0.01$), and no significance after APV application ($P > 0.99$). (*I*) Normalized plot of 1/CV^2 versus amplitude of Dcdc2$^{wt/wt}$ (black circle) versus Dcdc2$^{del2/del2}$ (red circle) cells. Dcdc2$^{del2/del2}$ neurons on average show presynaptic APV effect, falling below the red-dotted diagonal line. (*J*) Effects of APV application on first response amplitude in Dcdc2$^{wt/wt}$ (gray bars) and Dcdc2$^{del2/del2}$ (red bars) neurons. Student's *t*-test, Dcdc2$^{wt/wt}$: $t_9 = 1.36$, $P = 0.21$; Dcdc2$^{del2/del2}$: $t_{12} = 3.81$, $P < 0.05$. Open circles connected with lines indicate individual neurons. Dcdc2$^{wt/wt}$: $n = 10$ pairs, Dcdc2$^{del2/del2}$: $n = 13$ pairs. (*K*) Interaction graph showing the effect of APV on mean paired-pulse ratios measured in layer 4 excitatory neurons while stimulating the VB for Dcdc2$^{wt/wt}$ (black filled square) and Dcdc2$^{del2/del2}$ (red filled square). Repeated-measures ANOVA, genotype × APV application interaction: $F_{1,12} = 3.97$, $P = 0.07$. Followed by Bonferroni's multiple comparisons test, difference significant between Dcdc2$^{wt/wt}$ versus Dcdc2$^{del2/del2}$ before APV ($P = 0.62$), and no significance after APV application ($P = 0.21$). Open circles connected with lines indicate individual neurons (Dcdc2$^{wt/wt}$: gray, Dcdc2$^{del2/del2}$: light red). (*L*) Averages of normalized first EPSC amplitudes (EPSC after APV/EPSC before APV) in Dcdc2$^{wt/wt}$ (gray bar) and Dcdc2$^{del2/del2}$ (red bar) neurons. Student's *t*-test, $t_{12} = 0.72$, $P = 0.48$. Open circles indicate individual neurons. Dcdc2$^{wt/wt}$: $n = 7$, Dcdc2$^{del2/del2}$: $n = 7$. *$P < 0.05$, **$P < 0.01$, ns, $P > 0.05$.

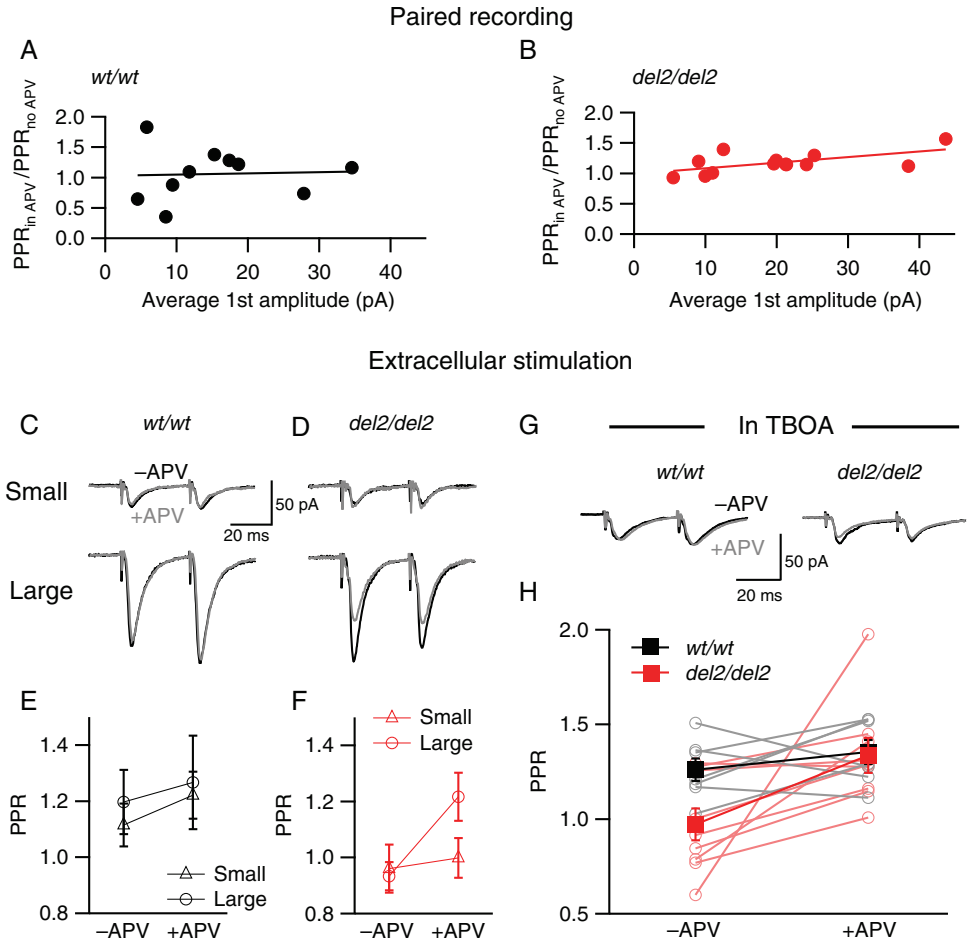

Figure 7. Effect of NMDAR blockade on release probability is enhanced when extracellular glutamate concentration is elevated by larger synaptic release or TBOA. Correlation between Effects of APV on PPR (PPR after APV/PPR before APV application) and average first EPSC amplitude of each postsynaptic cell recorded for (*A*) Dcdc2$^{wt/wt}$ and (*B*) Dcdc2$^{del2/del2}$ mice. PPR change and average first response amplitude are positively correlated in Dcdc2$^{del2/del2}$. Pearson's correlation, Dcdc2$^{wt/wt}$: $r = 0.05$, $P = 0.89$; Dcdc2$^{del2/del2}$: $r = 0.60$, $P < 0.05$. Dcdc2$^{wt/wt}$: $n = 9$ pairs, Dcdc2$^{del2/del2}$: $n = 13$ pairs. Representative EPSC pairs evoked by extrasynaptic electrical stimulation at minimal (top) versus high (bottom) intensities in a (*C*) Dcdc2$^{wt/wt}$ and a (*D*) Dcdc2$^{del2/del2}$ layer IV excitatory cell before (black) and after (gray) APV application. (*E*) Interaction graph showing mean PPR for small amplitude response (open triangle) and large amplitude response (open circle) before and after APV for Dcdc2$^{wt/wt}$ (black) cells. Two-way ANOVA, response amplitude × APV application interaction: $F_{1,9} = 3.14$, $P = 0.11$. Followed by Bonferroni's multiple comparisons test before versus after APV application, no significance for large ($P = 0.60$) or small amplitude ($P = 0.27$). (*F*) Interaction graph showing mean PPR for small amplitude response (open triangle) and large amplitude response (open circle) before and after APV for Dcdc2$^{del2/del2}$ (red) cells. Two-way ANOVA, response amplitude × APV application interaction: $F_{1,9} = 8.04$, $P < 0.05$. Followed by Bonferroni's multiple comparisons test before versus after APV application, difference significant for large amplitude response $P < 0.05$), no significance for small amplitude ($P = 0.99$). Dcdc2$^{wt/wt}$: $n = 10$; Dcdc2$^{del2/del2}$: $n = 10$. (*G*) Representative EPSCs of a Dcdc2$^{wt/wt}$ (left) and a Dcdc2$^{del2/del2}$ (right) layer IV neuron evoked by minimal stimulus intensity before (black) and after (gray) APV application, measured in 3 µM TBOA at room temperature. (*H*) Interaction graph showing mean PPRs for Dcdc2$^{wt/wt}$ (filled black square) and Dcdc2$^{del2/del2}$ (filled red square) cells before and after APV. Open circles connected with lines indicate individual neurons (Dcdc2$^{wt/wt}$: gray, Dcdc2$^{del2/del2}$: light red). Repeated-measures ANOVA, main effect of APV: $F_{1,14} = 6.70$, $P < 0.05$. Followed by Bonferroni's multiple comparisons test, difference significant between Dcdc2$^{wt/wt}$ and Dcdc2$^{del2/del2}$ before APV ($P < 0.05$); no significance after APV ($P > 0.05$). Dcdc2$^{wt/wt}$: $n = 7$, Dcdc2$^{del2/del2}$ $n = 9$.

When average response size and the change in paired-pulse ratio for each cell were compared, we found while, in wild types, amplitudes did not correlate with changes in paired-pulse ratio after applying APV, larger amplitudes correlated with larger changes in *Dcdc2* mutant neurons (Pearson correlation, Dcdc2$^{wt/wt}$: $P = 0.89$; Dcdc2$^{del2/del2}$: $P < 0.05$, Fig. 7*A*,*B*). This suggested that NMDAR activation by evoked release on presynaptic cells in the mutants is more pronounced when glutamate release amplitude is larger. Given this increased activation, we hypothesize that the additional NMDARs in mutants might be autoreceptors that can be activated with higher glutamate concentrations, revealing larger changes in paired-pulse ratio after APV application. To test whether the APV effect in mutants is glutamate release size-dependent, we adjusted extracellular stimulation intensity to evoke minimal responses or large responses in the same postsynaptic neuron. Small and large responses evoked by set intensities were assessed again after bath application of APV (Fig. 7*C*, *D*). While paired-pulse ratios of both small and large responses in the mutants were comparable pre- and post-APV, only large responses, but not small response paired-pulse ratios were affected by NMDAR block (2-way ANOVA, $F_{1,9} = 8.04$, $P < 0.05$, Bonferroni's multiple comparisons test, see legend, Fig. 7*F*), suggesting that the APV-sensitive EPSC component is more pronounced when more glutamate is released by multiple synapses. If additional glutamate arising from released glutamate accounts for enhanced APV effect in the large evoked responses, then we predicted that with minimum stimulation, addition of TBOA, which blocks amino acid transporters (Tzingounis and Nicoll 2004), should reveal an APV effect on PPR in Dcdc2 mutants. Indeed, in the presence of a low concentration of TBOA (3 µM), even small responses

in mutant synapses showed and APV sensitivity, returning them back to wild-type levels (repeated-measures ANOVA, $F_{1,14} = 6.70$, $P = 0.021$, Fig. 7*G*,*H*). These results indicate that during evoked synaptic release in mutants, NMDAR activation is enhanced in higher concentrations of glutamate, and this action is consistent with NMDARs activated by released glutamate "spilling over" to autoreceptors. We also noted that, for responses with amplitudes similar to extracellularly evoked small responses, paired recordings showed APV effects on PPR. This apparent discrepancy in small responses evoked by either paired recordings or minimal extracellular stimulation could be due to different populations of fibers recruited in extracellular minimum stimulation experiments where the presynaptic connection is not specified as in the paired intracellular recordings.

Finally, in an initial effort to determine whether the elevation in synaptic connectivity in somatosensory cortex may be relatable to a change in somatosensory-guided behavior, we compared wild-type and mutant animals in a novel stimulus recognition test designed to assess whisker-dependent texture discrimination. Although *Dcdc2* mutant mice and wild-type mice showed a high degree of variability in this task, the Dcdc2 mutants overall performed significantly worse than wild-type mice (Supplementary Fig. 1), suggesting preliminarily that Dcdc2 mutation impacts the ability of animals to either discriminate between different textures, or to keep in short-term memory a previously experienced somatosensory stimulus.

Discussion

In this study, we show that glutamatergic synaptic transmission is elevated in *Dcdc2* mutant mice, and this elevation is at least in part through an NMDAR-mediated, presynaptic mechanism at L4 synaptic connections. We have shown previously that increased NMDAR-mediated activity is the cause for degraded spike-time precision in Dcdc2 mutant mice (Che et al. 2013). The results of the present study suggest that the source of increased NMDAR activation that degrades spike-time precision may be through an increase in the probability of transmitter release, and but not by increased postsynaptic NMDARs. Elevated glutamate levels have been previously found in neurodevelopmental disorders including attention deficit/hyperactivity disorder (Carrey et al. 2007), autism (Brown et al. 2013), and most recently associated with individual differences in reading ability in emergent readers (Pugh et al. 2014). Similarly, evidence has accumulated that NMDARs at locations other than the PSD may play important roles in neuropathologies (Lipton 2006; Zhao 2006; Okamoto et al. 2009; Hardingham and Bading 2010; Talantova et al. 2013), which were previously attributed to postsynaptic NMDARs. In particular, presynaptic NMDAR dysfunction is found to be involved in epilepsy (Yang 2006), fetal alcohol spectrum disorder (Valenzuela et al. 2008), schizophrenia (Kristiansen et al. 2010), chronic pain (Zhao 2006), and spreading depression (Zhou et al. 2013). Findings from our study might provide a cellular basis, that is, increased presynaptic transmitter release, for previously reported neurofunctional and neurochemical changes associated with RD. The enhanced level of glutamate release caused by activated presynaptic NMDARs may result in elevated network excitability and synaptic noise fluctuations, both of which could lead to less precise neural encoding (Harsch and Robinson 2000; Chance et al. 2002; Ermentrout et al. 2008; Mozzachiodi and Byrne 2010; Centanni et al. 2013; Che et al. 2013).

Through pharmacological approaches, we demonstrated that NMDAR antagonism is effective in reducing the elevated release probability in *Dcdc2* mutants to wild-type levels. In addition, we showed that the NMDARs responsible for increased synaptic transmission are likely not located postsynaptically, since their function was not blocked by either hyperpolarizing the postsynaptic cell or by MK-801 injected intracellularly. Although the specific locus of expression of NMDARs that act presynaptically is still debated (review see Duguid (2013)), we argue that in the case of *Dcdc2* mutants, presynaptically localized NMDAR function is the most parsimonious explanation. First, we were unable to find evidence supporting any changes in postsynaptic NMDAR and AMPAR expression or function. Second, although electrotonic spread of somatodendritic NMDAR activation could also contribute to increased glutamate release in the mutant, we did not observe changes in mEPSC frequencies when RMPs were depolarized in wild-type L4 neurons, suggesting that depolarized membrane potential alone could not account for the altered synaptic release measured in mutants.

Elevated function of presynaptic NMDARs could either result from increased activation of receptors present or near presynaptic terminals or through increased numbers of functional NMDARs transported to presynaptic terminals in Dcdc2 mutants. Elevated function of presynaptic NMDARs could result from increased levels of glycine, or changes in glycine-gated NMDAR subunits. Glycine- gated NMDAR subunits NR2B and NR3CA have been shown to have developmentally regulated roles in presynaptic NMDAR function (Li et al. 2008; Larsen et al. 2011) and activation of these subunits could be responsible for the effects we observe in Dcdc2 mutants. In addition, given the likely role of Dcdc2 in cytoskeletal functions based on its molecular similarity to other members of the DCX family and its interaction with JIP1, a kinesin cargo adaptor, we hypothesize that *Dcdc2* regulates NMDAR protein trafficking to presynaptic terminals (Coquelle et al. 2006; Taylor et al. 2000). Future studies interrogating whether NR2B and or NR3A subunits are increased in their number and/or transport to presynaptic terminals in Dcdc2 mutants seems well justified.

In neocortex of developing animals, NMDARs located presynaptically are necessary for the induction of an important form of synaptic plasticity, cortical LTD (Sjöström et al. 2003; Bender et al. 2006; Corlew et al. 2007; Rodríguez-Moreno and Paulsen 2008). Interestingly, variants in *GRIN2B*, the gene coding for NR2B subunit, has been linked to weak performances in tasks involving short-term memory (Brkanac et al. 2008; Ludwig et al. 2009), and RD-related phenotypes (Mascheretti et al. 2014) in individuals with RD. *Dcdc2* mutant mice were shown to perform worse in short-term memory-based tactile discrimination tasks in our study (Supplementary Fig. 1), as well as spatial working memory tasks in previous studies (Gabel et al. 2011; Truong et al. 2014). These findings might suggest that the short-term memory deficits in *Dcdc2* mutants could be related to similar changes in NR2B-associated pathways as in RD individuals.

Whether other dyslexia-associated genes are associated with changes in glutamatergic transmission remains an open question. One other study showed that knockdown by shRNA of Kiaa0319 in rat auditory cortex increases the excitability of pyramidal neurons, but changes in synaptic activity were not thoroughly examined in that study (Centanni et al. 2013). Dyx1c1 and Robo1, the other 2 genes with replicated association to dyslexia (Kere 2014), have not yet been examined for their potential roles in cellular synaptic physiology. Identification of the molecular pathways through which *Dcdc2* regulates NMDAR presynaptic function and its developmental plasticity may lead to identification of new targets for understanding the genetic and/or environmental causes of RD.

Funding

This work was funded by grants from NIH/NICHD P01HD057853 and R01HD055655.

Notes

Conflict of Interest: None declared.

References

Agmon A, Connors BW. 1991. Thalamocortical responses of mouse somatosensory (barrel) cortex in vitro. Neuroscience. 41(2):365–379.

Agmon A, O'Dowd DK. 1992. NMDA receptor-mediated currents are prominent in the thalamocortical synaptic response before maturation of inhibition. J Neurophysiol. 68(1):345–349.

Bender KJ, Allen CB, Bender VA, Feldman DE. 2006. Synaptic basis for whisker deprivation-induced synaptic depression in rat somatosensory cortex. J Neurosci. 26(16):4155–4165.

Benshalom G, White EL. 1986. Quantification of thalamocortical synapses with spiny stellate neurons in layer IV of mouse somatosensory cortex. J Comp Neurol. 253(3):303–314.

Berretta N, Jones RS. 1996. Tonic facilitation of glutamate release by presynaptic N-methyl-D-aspartate autoreceptors in the entorhinal cortex. Neuroscience. 75(2):339–344.

Brasier DJ, Feldman DE. 2008. Synapse-specific expression of functional presynaptic NMDA receptors in rat somatosensory cortex. J Neurosci 28(9):2199–2211.

Brkanac Z, Chapman NH, Igo RP, Matsushita MM, Nielsen K, Berninger VW, et al. 2008. Genome scan of a nonword repetition phenotype in families with dyslexia: evidence for multiple loci. Behav Genet. 38(5):462–475.

Brown MS, Singel D, Hepburn S, Rojas DC. 2013. Increased glutamate concentration in the auditory cortex of persons with autism and first-degree relatives: a 1H-MRS study. Autism Res. doi:10.1002/aur.1260/full.

Burbridge TJ, Wang Y, Volz AJ, Peschansky VJ, Lisann L, Galaburda AM, et al. 2008. Postnatal analysis of the effect of embryonic knockdown and overexpression of candidate dyslexia susceptibility gene homolog Dcdc2 in the rat. Neuroscience. 152(3):723–733.

Carrey NJ, MacMaster FP, Gaudet L, Schmidt MH. 2007. Striatal creatine and glutamate/glutamine in attention-deficit/hyperactivity disorder. J Child Adolesc Psychopharmacol. 17(1):11–17.

Cartmell J, Schoepp DD. 2000. Regulation of neurotransmitter release by metabotropic glutamate receptors. J Neurochem. doi:10.1046/j.1471-4159.2000.0750889.x/full.

Centanni TM, Booker AB, Sloan AM, Sloan AM, et al. 2013. Knockdown of the dyslexia-associated gene Kiaa0319 impairs temporal responses to speech stimuli in rat primary auditory cortex. Cereb Cortex. 24(7):1753–1766.

Chance FS, Abbott LF, Reyes AD. 2002. Gain modulation from background synaptic input. Neuron. 35(4):773–782.

Che A, Girgenti MJ, Loturco J. 2013. The dyslexia-associated gene Dcdc2 is required for spike-timing precision in mouse neocortex. Biol Psychiatry. 76(5):387–396.

Chittajallu R, Vignes M, Dev KK, Barnes JM. 1996. Regulation of glutamate release by presynaptic kainate receptors in the hippocampus. Nature. 379(6560):78–81.

Clements J. 1997. Detection of spontaneous synaptic events with an optimally scaled template. Biophys J. 73(1):220–229.

Cope N, Eicher JD, Meng H, Gibson CJ, Hager K, Lacadie C, et al. 2012. Variants in the DYX2 locus are associated with altered brain activation in reading-related brain regions in subjects with reading disability. Neuroimage. 63(1):148–156.

Corlew R, Brasier DJ, Feldman DE, Philpot BD. 2008. Presynaptic NMDA receptors: newly appreciated roles in cortical synaptic function and plasticity. Neuroscientist. 14(6):609–625.

Corlew R, Wang Y, Ghermazien H, Erisir A, Philpot BD. 2007. Developmental switch in the contribution of presynaptic and postsynaptic NMDA receptors to long-term depression. J Neurosci. 27(37):9835–9845.

Couto JM, Gomez L, Wigg K, Ickowicz A, Pathare T, Malone M, et al. 2009. Association of attention-deficit/hyperactivity disorder with a candidate region for reading disabilities on chromosome 6p. Biol Psychiatry. 66(4):368–375.

Darki F, Peyrard-Janvid M, Matsson H, Kere J, Klingberg T. 2012. Three dyslexia susceptibility genes, DYX1C1, DCDC2, and KIAA0319, affect temporo-parietal white matter structure. Biol Psychiatry. 72(8):671–676.

Del Castillo J, Katz B. 1954. Statistical factors involved in neuromuscular facilitation and depression. J Physiol. 124(3):574.

Duguid IC. 2013. Presynaptic NMDA receptors: are they dendritic receptors in disguise? Brain Res Bull. 93:4–9.

Eicher JD, Gruen JR. 2013. Imaging-genetics in dyslexia: connecting risk genetic variants to brain neuroimaging and ultimately to reading impairments. Mol Genet Metab. 110(3):201–212.

Ermentrout GB, Galán RF, Urban NN. 2008. Reliability, synchrony and noise. Trends Neurosci. 31(8):428–434.

Faber D, Korn H. 1991. Applicability of the coefficient of variation method for analyzing synaptic plasticity. Biophys J. 60(5):1288–1294.

Feldman DE, Nicoll RA, Malenka RC, Isaac JT. 1998. Long-term depression at thalamocortical synapses in developing rat somatosensory cortex. Neuron. 21(2):347–357.

Feldmeyer D, Egger V, Lübke J, Sakmann B. 1999. Reliable synaptic connections between pairs of excitatory layer 4 neurones within a single "barrel" of developing rat somatosensory cortex. J Physiol. 521(Pt 1):169–190.

Freund TF, Katona I, Piomelli D. 2003. Role of endogenous cannabinoids in synaptic signaling. Physiol Rev. 83(3):1017–1066.

Gabel LA, Marin I, LoTurco JJ, Che A, Murphy C, Manglani M, et al. 2011. Mutation of the dyslexia-associated gene Dcdc2 impairs LTM and visuo-spatial performance in mice. Genes Brain Behav. 10(8):868–875.

Galaburda AM, Loturco J, Ramus F, Fitch RH, Rosen GD. 2006. From genes to behavior in developmental dyslexia. Nat Neurosci. 9(10):1213–1217.

Gil Z, Connors BW, Amitai Y. 1999. Efficacy of thalamocortical and intracortical synaptic connections: quanta, innervation, and reliability. Neuron. 23(2):385–397.

Hardingham GE, Bading H. 2010. Synaptic versus extrasynaptic NMDA receptor signalling: implications for neurodegenerative disorders. Nat Rev Neurosci. 11(10):682–696.

Harsch A, Robinson H. 2000. Postsynaptic variability of firing in rat cortical neurons: the roles of input synchronization and synaptic NMDA receptor conductance. J Neurosci. 20(16):6181–6192.

Hull C, Isaacson JS, Scanziani M. 2009. Postsynaptic mechanisms govern the differential excitation of cortical neurons by thalamic inputs. J Neurosci. 29(28):9127–9136.

Jamadar S, Powers NR, Meda SA, Calhoun VD, Gelernter J, Gruen JR, et al. 2012. Genetic influences of resting state fMRI activity in language-related brain regions in healthy controls

and schizophrenia patients: a pilot study. Brain Imaging Behav. 7(1):15–27.

Karim F, Wang CC, Gereau RW. 2001. Metabotropic glutamate receptor subtypes 1 and 5 are activators of extracellular signal-regulated kinase signaling required for inflammatory pain in mice. J Neurosci. 21(11):3711–3719.

Kere J. 2014. The molecular genetics and neurobiology of developmental dyslexia as model of a complex phenotype. Biochem Biophys Res Commun. 452(2):236–243.

Kreitzer AC, Carter AG, Regehr WG. 2002. Inhibition of interneuron firing extends the spread of endocannabinoid signaling in the cerebellum. Neuron. 34(5):787–796.

Kristiansen LV, Bakir B, Haroutunian V, Meador-Woodruff JH. 2010. Expression of the NR2B-NMDA receptor trafficking complex in prefrontal cortex from a group of elderly patients with schizophrenia. Schizophr Res. 119(1–3):198–209.

Kunz PA, Roberts AC, Philpot BD. 2013. Presynaptic NMDA receptor mechanisms for enhancing spontaneous neurotransmitter release. J Neurosci. 33(18):7762–7769.

Larsen RS, Corlew RJ, Henson MA, Roberts AC, Mishina M, Watanabe M, et al. 2011. NR3A-containing NMDARs promote neurotransmitter release and spike timing–dependent plasticity. Nat Neurosci. 14(3):338–344.

Li Y-H, Han T-Z, Meng K. 2008. Tonic facilitation of glutamate release by glycine binding sites on presynaptic NR2B-containing NMDA autoreceptors in the rat visual cortex. Neurosci Lett. 432(3):212–216.

Lipton SA. 2006. Paradigm shift in neuroprotection by NMDA receptor blockade: memantine and beyond. Nat Rev Drug Discov. 5(2):160–170.

Ludwig KU, Roeske D, Herms S, Schumacher J, Warnke A, Plume E, et al. 2009. Variation in GRIN2Bcontributes to weak performance in verbal short-term memory in children with dyslexia. Am J Med Genet. 9999B:n/a–n/a.

Magdaleno S, Jensen P, Brumwell CL, Seal A, Lehman K, Asbury A, et al. 2006. BGEM: an in situ hybridization database of gene expression in the embryonic and adult mouse nervous system. PLos Biol. 4(4):e86.

Malinow R, Tsien RW. 1990. Presynaptic enhancement shown by whole-cell recordings of long-term potentiation in hippocampal slices. Nature. 346(6280):177–180.

Manabe T, Wyllie D, Perkel D, Nicoll RA. 1993. Modulation of synaptic transmission and long-term potentiation: effects on paired pulse facilitation and EPSC variance in the CA1 region of the hippocampus. J Neurophysiol. 70(4):1451–1459.

Marino C, Mascheretti S, Riva V, Cattaneo F. 2011. Pleiotropic effects of DCDC2 and DYX1C1 genes on language and mathematics traits in nuclear families of developmental dyslexia. Behav Genet. 41(1):67–76.

Marino C, Meng H, Mascheretti S, Rusconi M, Cope N, Giorda R, Molteni M, Gruen JR. 2012. DCDC2 genetic variants and susceptibility to developmental dyslexia. Psychiatr Genet. 22 (1):25–30.

Mascheretti S, Facoetti A, Giorda R, Beri S, Riva V, Trezzi V, et al. 2014. GRIN2B mediates susceptibility to intelligence quotient and cognitive impairments in developmental dyslexia. Psychiatr Genet. 25(1):19–20.

McGuinness L, Taylor C, Taylor RDT, Yau C, Langenhan T, Hart ML, et al. 2010. Presynaptic NMDARs in the hippocampus facilitate transmitter release at theta frequency. Neuron. 68 (6):1109–1127.

Meda SA, Gelernter J, Gruen JR, Calhoun VD, Meng H, Cope NA, et al. 2008. Polymorphism of DCDC2 reveals differences in cortical morphology of healthy individuals-a preliminary voxel based morphometry study. Brain Imaging Behav. 2 (1):21–26.

Meng H, Smith SD, Hager K, Held M, Liu J, Olson RK, et al. 2005. DCDC2 is associated with reading disability and modulates neuronal development in the brain. Proc Natl Acad Sci USA. 102(47):17053–8.

Mozzachiodi R, Byrne JH. 2010. More than synaptic plasticity: role of nonsynaptic plasticity in learning and memory. Trends Neurosci. 33(1):17–26.

Myme C, Sugino K. 2003. The NMDA-to-AMPA ratio at synapses onto layer 2/3 pyramidal neurons is conserved across prefrontal and visual cortices. J Neurophysiol. 90(2):771–779.

Okamoto S-I, Pouladi MA, Talantova M, Yao D, Xia P, Ehrnhoefer DE, et al. 2009. Balance between synaptic versus extrasynaptic NMDA receptor activity influences inclusions and neurotoxicity of mutant huntingtin. Nat Med. 15 (12):1407–1413.

Petersen CCH, Sakmann B. 2000. The excitatory neuronal network of rat layer 4 barrel cortex. J Neurosci. 20(20):7579–7586.

Peterson RL, Pennington BF. 2012. Developmental dyslexia. Lancet. 379(9830):1997–2007.

Porter JT, Johnson CK, Agmon A. 2001. Diverse types of interneurons generate thalamus-evoked feedforward inhibition in the mouse barrel cortex. J Neurosci. 21(8):2699–2710.

Pugh KR, Frost SJ, Rothman DL, Hoeft F, Del Tufo SN, Mason GF, et al. 2014. Glutamate and choline levels predict individual differences in reading ability in emergent readers. J Neurosci. 34 (11):4082–4089.

Ramus F. 2003. Developmental dyslexia: specific phonological deficit or general sensorimotor dysfunction? Curr Opin Neurobiol. 13(2):212–218.

Raschle NM, Stering PL, Meissner SN, Gaab N. 2013. Altered neuronal response during rapid auditory processing and its relation to phonological processing in prereading children at familial risk for dyslexia. Cereb Cortex. 24(9):2489–2501.

Rodríguez-Moreno A, Paulsen O. 2008. Spike timing-dependent long-term depression requires presynaptic NMDA receptors. Nat Neurosci. 11(7):744–745.

Rosenberg J, Pennington BF, Willcutt EG, Olson RK. 2012. Gene by environment interactions influencing reading disability and the inattentive symptom dimension of attention deficit/hyperactivity disorder. J Child Psychol Psychiatry. 53 (3):243–251.

Schubert D, Kötter R, Zilles K, Luhmann HJ, Staiger JF. 2003. Cell type-specific circuits of cortical layer IV spiny neurons. J Neurosci. 23(7):2961–2970.

Schumacher J, Anthoni H, Dahdouh F, König IR, Hillmer AM, Kluck N, et al. 2006. Strong genetic evidence of DCDC2 as a susceptibility gene for dyslexia. Am J Hum Genet. 78(1): 52–62.

Sjöström P, Turrigiano G, Nelson SB. 2003. Neocortical LTD via coincident activation of presynaptic NMDA and cannabinoid receptors. Neuron. 39(4):641–654.

Takahashi T, Kajikawa Y, Tsujimoto T. 1998. G-Protein-coupled modulation of presynaptic calcium currents and transmitter release by a GABAB receptor. J Neurosci. 18(9):3138–3146.

Talantova M, Sanz-Blasco S, Zhang X, Xia P, Akhtar MW, Okamoto S-I, et al. 2013. Aβ induces astrocytic glutamate release, extrasynaptic NMDA receptor activation, and synaptic loss. Proc Natl Acad Sci USA. 110(27):E2518–E2527.

Truong DT, Che A, Rendall AR, Szalkowski CE, LoTurco JJ, Galaburda AM, et al. 2014. Mutation of Dcdc2in mice leads to impairments in auditory processing and memory ability. Genes Brain Behav. n/a–n/a. doi:10.1111/gbb.12170.

Turecek R, Trussell LO. 2001. Presynaptic glycine receptors enhance transmitter release at a mammalian central synapse. Nature. 411(6837):587–590.

Tzingounis AV, Nicoll RA. 2004. Presynaptic NMDA receptors get into the act. Nat Neurosci. 7(5):419–420.

Tzounopoulos T, Rubio ME, Keen JE, Trussell LO. 2007. Coactivation of pre- and postsynaptic signaling mechanisms determines cell-specific spike-timing-dependent plasticity. Neuron. 54(2):291–301.

Valenzuela CF, Partridge LD, Mameli M, Meyer DA. 2008. Modulation of glutamatergic transmission by sulfated steroids: role in fetal alcohol spectrum disorder. Brain Res Rev. 57 (2):506–519.

Yang J. 2006. Tonic facilitation of glutamate release by presynaptic NR2B-containing NMDA receptors is increased in the entorhinal cortex of chronically epileptic rats. J Neurosci. 26 (2):406–410.

Zhao MG. 2006. Enhanced presynaptic neurotransmitter release in the anterior cingulate cortex of mice with chronic pain. J Neurosci. 26(35):8923–8930.

Zhou N, Rungta RL, Malik A, Han H, Wu DC, MacVicar BA. 2013. Regenerative glutamate release by presynaptic NMDA receptors contributes to spreading depression. J Cereb Blood Flow Metab. 33(10):1582–1594.

Zucker RS, Regehr WG. 2002. Short-term synaptic plasticity. Ann Rev Physiol. 64:355–405.